Thermal Stabilization of the Catalytic Domain of Botulinum Neurotoxin E by Phosphorylation of a Single Tyrosine Residue†

Clara Blanes-Mira,‡ Cristina Ibañez,‡ Gregorio Fernández-Ballester,‡ Rosa Planells-Cases,‡ Enrique Pérez-Payá,§ and Antonio Ferrer-Montiel*,‡

Centro de Biología Molecular y Celular, Universidad Miguel Hernández, Alicante, Spain, and Departamento de Bioquímica y Biología Molecular, Universidad de Valencia, Valencia, Spain

Received August 14, 2000; Revised Manuscript Received November 6, 2000

ABSTRACT: The catalytic domain of clostridial neurotoxins is a substrate of tyrosine-specific protein kinases. The functional role of tyrosine phosphorylation and also the number and location of its (their) phosphorylation site(s) are yet elusive. We have used the recombinant catalytic domain of botulinum neurotoxin E (BoNT E) to examine these issues. Bacterially expressed and purified BoNT E catalytic domain was fully active, and was phosphorylated in vitro by the tyrosine-specific kinase Src. Tyrosine phosphorylation of the catalytic domain increased the protein thermal stability without affecting its proteolytic activity. Covalent modification of the endopeptidase promoted a disorder-to-order transition, as evidenced by the 35% increment of the α-helical content, which resulted in a 4 °C increase of its denaturation temperature. Site-directed replacement of tyrosine at position 67 completely abolished phosphate incorporation by Src. Constitutively unphosphorylated endopeptidase mutants exhibited functional properties virtually identical to those displayed by the nonphosphorylated wild-type catalytic domain. These findings indicate the presence of a single phosphorylation site in the catalytic domain of clostridial neurotoxins, and that its covalent modification primarily modulates the protein thermostability.

Botulinum neurotoxins (BoNTs)[1] are potent neuroparalytic agents secreted by *Clostridium botulinum* (*1*). BoNTs block cholinergic neurotransmission at the neuromuscular junction, thereby causing flaccid and spastic paralysis (*1*−*3*). This property is currently being used to ameliorate the symptomatology of spasmodic disorders such as dystonias (*4*). The seven distinct BoNT serotypes (A−G) are soluble proteins, produced as single chains of 150 kDa (*1*−*3*). The holotoxin undergoes proteolytic cleavage, yielding a fully active dichain polypeptide composed of a heavy chain (HC) of 100 kDa and a light chain (LC) of 50 kDa, linked by a disulfide bond. Reduction of the disulfide separates the LCs and HCs, which are devoid of neurotoxic activity in conventional assays (*1*). The LCs of this family of neurotoxins, as well as that of the structurally related tetanus neurotoxin (TeNTx), are Zn^{2+}-dependent endopeptidases that selectively truncate SNARE proteins, thus inhibiting Ca^{2+}-dependent exocytosis in synaptic terminals (*2, 3, 5*−*9*). Because of its proteolytic activity, the LC is also known as the catalytic domain.

Clostridial neurotoxins are substrates of tyrosine-specific kinases such as Src, which phosphorylates both the HC and LC (*10*). Tyrosine phosphorylation appears to be a common covalent modification of botulinum and tetanus neurotoxins, suggesting the presence of a conserved structural motif containing the phosphate acceptor site(s) (*10*). Covalent modification of BoNT A and E holotoxins results in prominent augmentation of their catalytic activity by achieving maximal substrate cleavage at lower neurotoxin concentrations and shorter reaction times (*10*). In addition, tyrosine phosphorylation of these neurotoxins promotes a structural change in the protein by increasing the α-helical content with a concomitant decrease of less ordered structures such as turns and random coils (*11*). The phosphorylation-induced structural change provokes a significant stabilization of the folded proteins (*11*). The remarkable functional and structural effects of botulinum neurotoxin phosphorylation point to the phosphorylated form as the biologically relevant neurotoxin (*10*).

Because both neutoroxin chains are readily phosphorylated in tyrosine residues, it is plausible that the reported phosphorylation-induced structure−function regulation of the catalytic domain may have been significantly influenced by the presence of the HC (*10, 11*). Accordingly, the role of tyrosine phosphorylation of the catalytic domain as well as the identity of its tyrosine phosphorylation sites remains unknown. Here, we have used the recombinant, purified BoNT E catalytic domain to address these questions. We

† This work was supported by grants from the Generalitat Valenciana (GVA 98-5-31) Comisión Interministerial de Ciencia y Tecnología (CICYT-PETRI, 95-0388-OP) to A.F.-M.

* To whom correspondence should be addressed at the Centro de Biología Molecular y Celular, Universidad Miguel Hernández, Edif. Torregaitán, Avda. Ferrocarril s/n, 03202 Elche, Spain. Phone: +34-96 665 8727, Fax: +34-96 665 8758, email: aferrer@umh.es.

‡ Universidad Miguel Hernández.

§ Universidad de Valencia.

[1] Abbreviations: BoNT, botulinum neurotoxin; LC, light chain/catalytic domain; HC, heavy chain; CD, circular dichroism; DTT, dithiothreitol; GST, glutathione-*S*-transferase; IPTG, isopropyl-β-thiogalactoside; OG, *n*-octyl-β-D-glucopyranoside; TeNT, tetanus neurotoxin.

10.1021/bi001919y CCC: $20.00
Published on Web 01/26/2001

1	BONT/E	^{61}KNGDS-S**Y**YDP^{70}	^{299}KDVFEAK**Y**GL^{308}
2	BONT/A	^{65}KQVPV-S**Y**YDS^{74}	^{313}KNVFKEK**Y**LL^{322}
3	BONT/B	^{65}FNRDVCE**Y**YDP^{75}	^{320}KNKFKDK**Y**KF^{329}
4	BONT/G	^{65}FSKDVYE**Y**YDP^{75}	^{319}KQIYKNK**Y**DF^{328}
5	BONT/F	^{66}KNGSS-A**Y**YDP^{75}	^{317}KDYFQWK**Y**GL^{326}
6	BONT/C1	^{65}SPKSG--**Y**YDP^{73}	^{322}KQKLIRK**Y**RF^{331}
7	BONT/D	^{66}SKYQS--**Y**YDP^{74}	^{323}KKIFSEK**Y**NF^{332}
8	TETX	^{65}IEGAS-E**Y**YDP^{74}	^{322}KQIYQQK**Y**QF^{331}

FIGURE 1: Potential tyrosine phosphorylation sites on the clostridial neurotoxin catalytic domain. Amino acid alignment of putative tyrosine kinase consensus sequences in BoNT and TeNT LCs (*32*). Black shaded amino acids indicate the potential phosphate acceptor sites. Numbers indicate residue location in the catalytic domain sequence.

show that the recombinant endopeptidase is a substrate of the tyrosine-specific kinase Src. At variance with native LC, covalent modification of the recombinant enzyme did not alter its proteolytic activity. In contrast, tyrosine-phosphorylated recombinant BoNT E catalytic domain exhibited a significant increase of the α-helical content and a conspicuous increment of its denaturing temperature. Amino acid sequence analysis revealed the presence of two distinct, highly conserved consensus recognition motifs for tyrosine kinases in the catalytic domain primary sequence, namely, residues 61−70 and 299−308 (*12*) (Figure 1). Site-directed mutagenesis demonstrated that tyrosine at position 67 is the phosphorylation site. Mutation of this residue to phenylalanine produced endopeptidase mutants that were not modified by Src, and exhibited biological properties akin to those characteristic of the nonphosphorylated wild-type enzyme.

EXPERIMENTAL PROCEDURES

Site-Specific Mutagenesis of the BoNT E Catalytic Domain. A cDNA plasmid encoding the BoNT E LC [kindly provided by Dr. H. Niemann (*13*)] was cloned into the pGEX-KG vector to obtain a glutathione-*S*-transferase (GST)−BoNT E LC fusion construct containing a thrombin cleavage site after the GST. Site-directed mutagenesis was carried out by generating PCR fragments using pairs of complementary mutant primers as described (*14*, *15*). BoNT E LC mutant sequences were verified by automated DNA sequencing. For the single mutants, the number indicates the position of the residue in the protein sequence, and the first letter is the natural amino acid in the wild-type protein and the second is the residue that substitutes it. Double mutants are denoted by their point mutations separated by a slash (/).

Expression and Purification of Recombinant BoNT E Catalytic Domain Species and SNAP-25. Recombinant BoNT E catalytic domain (rBoNT E LC) and SNAP-25 (rSNAP-25) were expressed in the *E. coli* strains M15pREP4 and BL21DE3, respectively. Protein expression was induced with 1 mM IPTG for 5 h at 30 °C. Bacterial cultures were pelleted, washed with lysis buffer (10 mM phosphate, pH 7.4, 136 mM NaCl, 2.7 mM KCl), digested with 0.1 mg/mL lysozyme for 10 min at 22 °C in lysis buffer, supplemented with 2 mM PMSF, 5 mM iodoacetamide, 5 mM EDTA, and sonicated (3 × 45 s) in a Branson 250 sonifier at 4 °C. Lysates were solubilized with 1% Triton X-100 for 20 min at 4 °C and cleared by centrifugation at 20000*g* for 30 min at 4 °C. GST−BoNT E LC and GST−SNAP-25 fusion proteins were present primarily as soluble fractions in the supernatant. Recombinant proteins were purified by affinity chromatography on glutathione−agarose (Pharmacia) following manufacturer's instructions. Purification of rBoNT E LC was carried out in 20 mM Hepes, pH 8.5, 0.4% *N*-lauroylsarcosine, 500 mM NaCl, 200 mM urea, 1 mM dithiothreitol (DTT), 2% Triton X-100. The use of detergents and urea prevented unspecific binding of the recombinant protein to the glutathione-conjugated agarose resin. Purification of rSNAP-25 was performed in 20 mM Hepes, pH 7.4, 100 mM NaCl, 0.05% *n*-octyl-β-D-glucopyranoside (OG), 5 mM DTT. Resin-bound fusion proteins were released by digestion with thrombin protease (Pharmacia) for 5 h at 23 °C. rBoNT E LC was extensively dialyzed into the 20 mM Hepes, pH 7.4, 0.05% OG buffer and rSNAP-25 into the 20 mM Hepes, pH 7.4, 80 mM KCl, 20 mM NaCl, 0.1% OG buffer. Proteins concentration was assayed with the BCA kit (Pierce), and purity was verified by gel analysis.

Phosphorylation of rBoNT E LC Species. Recombinant BoNT E LC species were tyrosine-phosphorylated as described (*10*). Briefly, 0.5 μM rBoNT E LC was incubated with 9 units of recombinant Src kinase (Upstate Biotecnology Inc.) in 20 mM Hepes, pH 7.4, 20 mM $MgCl_2$, 1 mM EGTA, 2 mM DTT, 0.5 mM ATP. Unphosphorylated neurotoxins refer to samples in which ATP was omitted but were subjected to the same treatments as phosphorylated samples. Reactions proceeded at 30 °C for the indicated times, and were terminated by addition of SDS−PAGE sample buffer or a Src inhibitor (*10*). Phosphorylation was analyzed by western immunoblot using a specific anti-phosphotyrosine monoclonal antibody (Sigma). Protein bands were electrotransferred onto nitrocellulose membranes and blocked with 3% bovine serum albumin. Bands were visualized using the alkaline phosphatase strategy (BioRad).

Endopeptidase Activity of rBoNT E LC Species. The endopeptidase activity of rBoNT E LC species was assayed in vitro using rSNAP-25. Cleavage assay was performed in a final volume of 20 μL [20 mM Hepes, pH 7.4, 2 mM DTT, 10 μM $Zn(CH_3COO)_2$], containing the recombinant catalytic domain and the substrate at the indicated concentrations and reaction times. Cleavage reactions were carried out at 23 °C. The extent of rSNAP-25 truncation was evaluated by SDS−PAGE on 12% gels. Proteolytic activity was determined by the change in the apparent mobility of the major product from 25 to 21.3 kDa (*2*, *6*, *10*). SDS−PAGE gels were digitized and quantified as described (*10*). For enzyme kinetics analysis, the velocity of rSNAP-25 cleavage was estimated during the first 10 min of the reaction. Lineweaver−Burk plots were used to estimate the K_M and V_{max} values (*16*).

Circular Dichroism Spectroscopy. Circular dichroism (CD) was carried out in a JASCO J-810 spectropolarimeter equipped with a computer-controlled temperature cuvette holder. CD data for the far-UV CD spectra (region 195−250 nm) were recorded with a 1 mm path length cell containing 3 μM protein in 10 mM Tris-HCl, pH 7.4, 0.05% OG. All spectra were recorded at 16 °C and at 50 nm/min (response time of 1 s), averaged (5 scans), and corrected for the buffer contribution. CD signals (in millidegrees) were converted to mean ellipticity (θ, mdeg cm^2 dmol^{-1}) using the relationship: $\theta_v = 100 \times$ CD signal/*CNl*, were *C* denotes the protein concentration, *N* the number of residues, and *l*

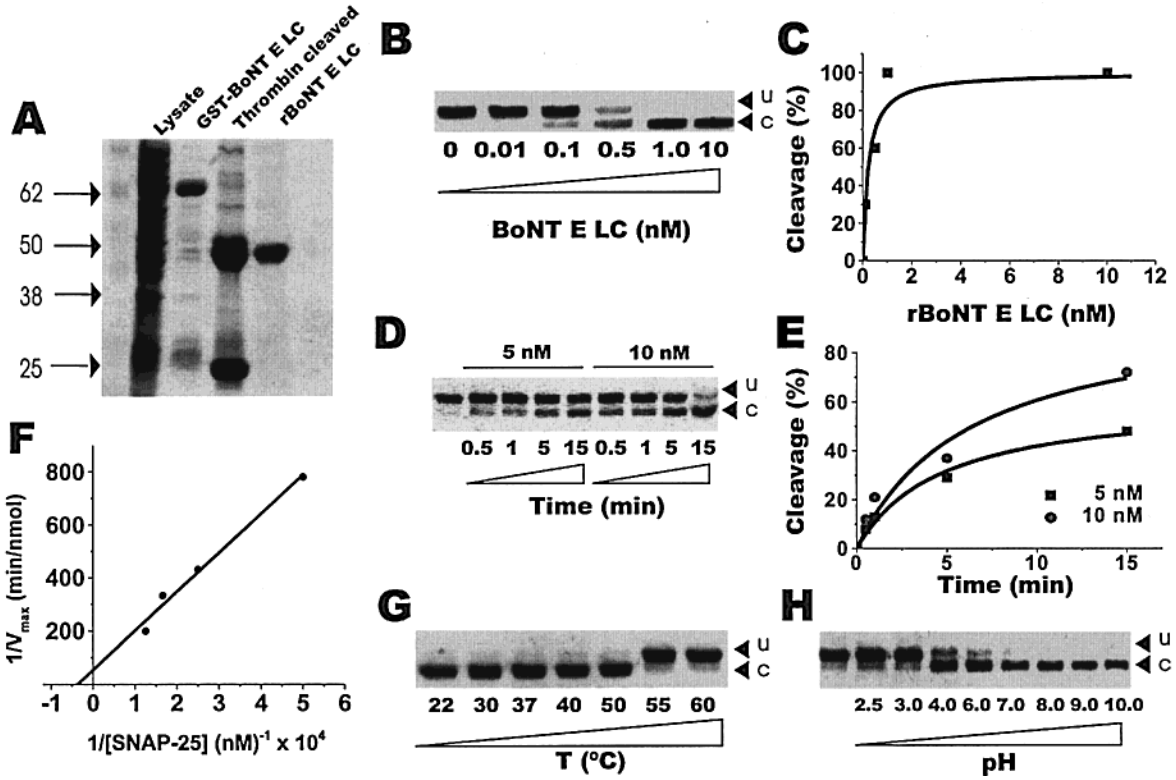

FIGURE 2: Recombinant BoNT E catalytic domain is a fully active endopeptidase. (A) SDS−PAGE analysis of the expression and purification of BoNT E LC in *E. coli*. Numbers on the left indicate molecular mass markers (kDa). (B) Cleavage of rSNAP-25 by recombinant BoNT E LC as a function of endopeptidase concentration. (C) Extent of rSNAP-25 proteolysis as a function of enzyme concentration quantified by image analysis of the SDS−PAGE gel shown in panel B. (D) Truncation of rSNAP-25 as a function of reaction time measured at two endopeptidase concentrations. (E) Kinetics of rSNAP-25 cleavage at two BoNT E LC concentrations. (F) Lineweaver−Burk analysis of enzyme kinetics. The solid line indicates the best fit to a linear regression. The K_M and V_{max} values were obtained from the *x*-intercept when $y = 0$ and the *y*-intercept at $x = 0$, respectively. (G) Temperature dependence of BoNT E LC proteolytic activity. Recombinant endopeptidase was incubated at the indicated temperatures for 60 min prior to the addition of rSNAP-25. (H) pH dependence of BoNT E LC enzymatic activity. Truncation of rSNAP-25 was evaluated at the indicated pH values; u and c denote uncleaved and cleaved rSNAP-25, respectively. Cleavage reactions proceeded for 60 min at 23 °C. rSNAP-25 concentration was 6 μM. The first lanes in panels D and H denote rSNAP-25 in the absence of enzyme. Other conditions as described under Experimental Procedures.

the path length. Protein concentration was verified by OD measurements at 280 nm using $\epsilon = 38\,780$ M^{-1} cm^{-1} (Antheprot 2000 V5.0 software package) (*17*). Secondary structure elements were inferred by fitting the CD spectra (*18*). Thermal denaturing experiments were carried out by monitoring the CD signal at 222 nm as a function of the temperature. The temperature was increased from 30 to 70 °C with a heat rate of 1 °C/min. The normalized molar ellipticity at 222 nm was plotted as a function of the temperature, and the experimental data were described by the logistic equation (*11*):

$$\frac{\theta}{\theta_{max}} = \frac{1}{1 + (T/T_d)^n}$$

where θ and θ_{max} denote the molar ellipticity and maximal θ at $\lambda = 222$ nm, respectively, n is the slope of the sigmoid, T is the temperature, and T_d is the denaturing temperature. Experimental points were fitted to the logistic equation with a nonlinear least-squares regression algorithm using MicroCal ORIGIN version 6.0.

RESULTS

Expression and Purification of the Fully Functional Recombinant BoNT E Catalytic Domain. To study the functional relevance of tyrosine phosphorylation of the BoNT E catalytic domain and to unravel its phosphate acceptor sites, we first expressed and purified rBoNT E LC using a GST strategy. The cDNA encoding the BoNT E catalytic domain was cloned as a GST−BoNT E LC fusion protein containing a cleavage site for thrombin. The GST fusion protein was expressed in *E. coli* strain M15pREP4 and its biosynthesis induced with IPTG (*19*). As illustrated in Figure 2A, IPTG-induced bacterial lysates exhibited a protein band with an apparent mobility of 62 kDa (Figure 2A, lane 1), which was specifically retained in a glutathione affinity chromatography column (Figure 2A, lane 2). Treatment with thrombin truncated the 62 kDa protein into two smaller polypeptides of 48 and 23 kDa (Figure 2A, lane 3), corresponding to rBoNT E LC and GST as evidenced by western immunoblotting (data not shown). This GST-based strategy produced up to 1 mg/L of bacterial culture of fairly homogeneous preparations of rBoNT E catalytic domain (Figure 2A, lane 4).

We next investigated if purified recombinant catalytic domain retained the proteolytic activity characteristic of its native counterpart by examining the efficiency of rSNAP-25 cleavage by the recombinant enzyme. Incubation of the substrate with increasing concentrations of rBoNT E LC at 23 °C for 60 min yielded complete cleavage of rSNAP-25 at [rBoNT E LC] ≥ 1 nM (Figure 2B). The estimated concentration of recombinant neurotoxin needed to truncate

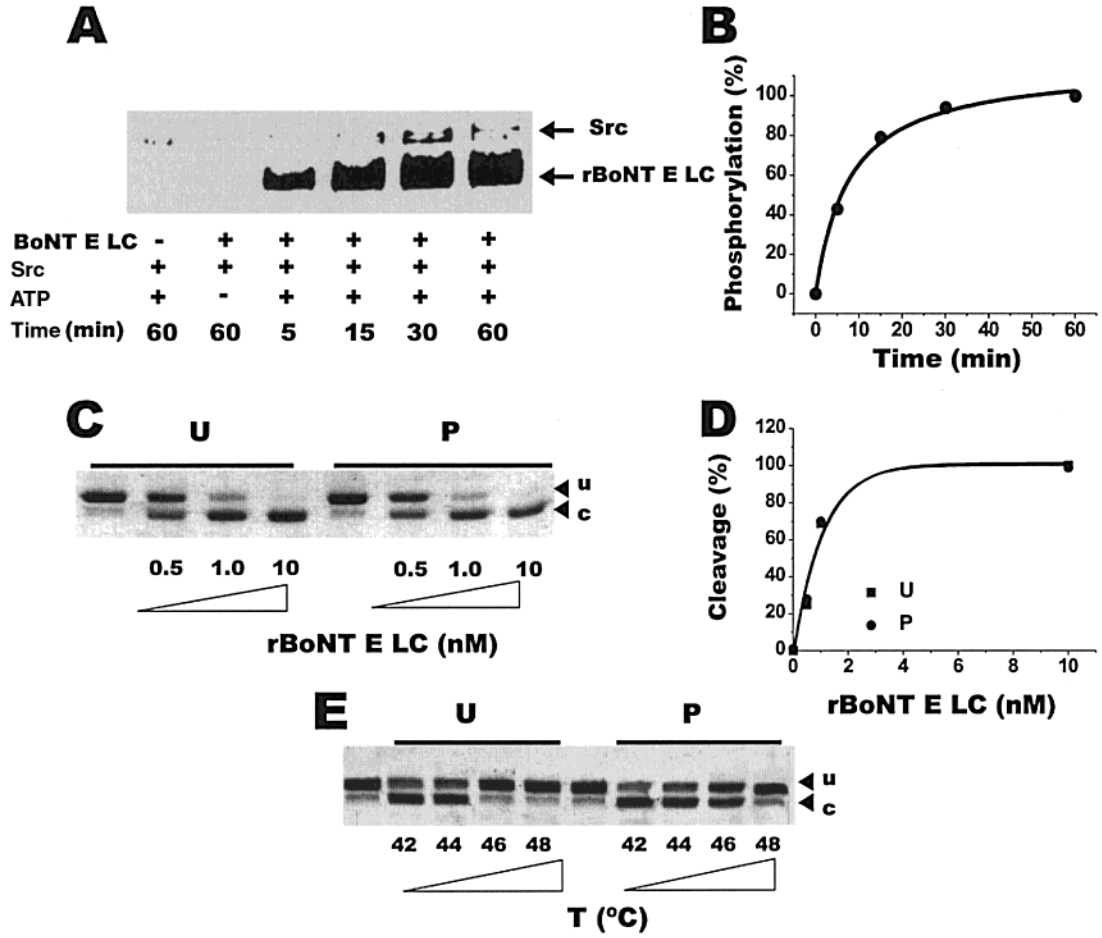

FIGURE 3: Tyrosine phosphorylation of the recombinant BoNT E catalytic domain. (A) Tyrosine-specific Src kinase phosphorylates the BoNT E LC. Tyrosine phosphorylation was evaluated by western immunoblotting using a monoclonal anti-phosphotyrosine antibody. Phosphorylation reaction was carried out at 30 °C using 9 units of kinase and 10 nM BoNT E LC. (B) The extent of tyrosine phosphorylation by Src was quantified from the digitized immunoblot shown in panel A by image analysis. (C) Cleavage of rSNAP-25 by unphosphorylated (U) and tyrosine-phosphorylated (P) BoNT E LC as a function of enzyme concentration. The reaction proceeded for 60 min at 23 °C. (D) Extent of rSNAP-25 cleavage as a function of BoNT E LC quantified by image analysis of the gel shown in panel B. (E) Thermal inactivation of the proteolytic activity of unphosphorylated and phosphorylated BoNT E LC. The catalytic domain (10 nM) was phosphorylated for 60 min at 30 °C with 9 units of Src kinase and incubated for 60 additional min at the indicated temperatures prior to the 5 min cleavage reaction at 23 °C. Substrate concentration was 6 μM. Unphosphorylated BoNT E LC (ATP omitted) was subjected to the same treatments as phosphorylated samples. First and fifth lanes in panel C, and first and sixth lanes in panel E, denote rSNAP-25 in the absence of enzyme.

half of the maximal substrate concentration was 0.3 nM (Figure 2C), which appears to be significantly lower than that reported for DTT-reduced native holotoxin (*10*). It should be noted that this apparent dissimilarity in EC_{50} values may result from differences in the concentration of the catalytic domain since the proteolytic activity of the native neurotoxin was studied as a function of the holotoxin concentration rather than that of the LC (*10*).

The kinetics of rSNAP-25 cleavage increased as the neurotoxin concentration was raised (Figure 2D). Complete cleavage of rSNAP-25 was accelerated from $t > 15$ min to $t \leq 15$ min when the [rBoNT E LC] was augmented from 5 to 10 nM (Figure 2E). A Lineweaver−Burk analysis of the enzyme kinetics yielded a K_M value of 27 μM, a V_{max} of 0.02 nmol/min, and a k_{cat} of 100 min^{-1} (Figure 2F). These enzyme kinetic parameters are similar to those reported for the catalytic domain of BoNT A (*20*).

To further characterize the properties of the catalytic domain, we studied the thermal stability (Figure 2G) and pH dependency of its proteolytic activity (Figure 2H). Preincubation of the rBoNT E LC at temperatures ranging from 22 to 60 °C for 60 min caused a complete loss of catalytic activity at $T \geq 55$ °C. Likewise, BoNT E LC-mediated cleavage of rSNAP-25 was abolished when the neurotoxin was challenged with pH ≤3.0 for 60 min. Taken together, these results indicate that the recombinant BoNT E catalytic domain is a fully active enzyme with functional properties comparable to those reported for native clostridial and tetanus neurotoxins (*20*−*23*).

The rBoNT E Catalytic Domain Is Phosphorylated by the Tyrosine-Specific Kinase Src. Tyrosine phosphorylation is a prominent covalent modification of both the HC and the LC (*10*). We assessed whether the rBoNT E LC was a substrate of Src, a tyrosine-specific kinase. Incubation of rBoNT E LC in the presence of Src and ATP at 30 °C resulted in the conspicuous incorporation of phosphate groups into tyrosine residues, as evidenced by immunoblot analysis using an anti-phosphotyrosine monoclonal antibody (Figure 3A). Note that the faint band of ≈55 kDa corresponds to Src autophosphorylation (Figure 3A, lane 1). Tyrosine phosphorylation was absent when ATP was omitted from the reaction (Figure 3A, lane 2). The extent of neurotoxin phosphorylation was time-dependent, exhibiting an apparent half-maximum of ≤5 min (Figure 3A,B), and saturation at

Table 1: Modulation of Clostridial Holotoxin and Catalytic Domain by Tyrosine Phosphorylation[a]

	proteolytic activity		protein structure and stability	
	[BoNT E] (nM)	t (min)	α-helical content	T_d (°C)
unphosphorylated				
holotoxin[b]	25 ± 3	40 ± 5	26	51 ± 0.3
catalytic domain	0.6 ± 0.2	12 ± 4	18	47 ± 0.2
phosphorylated				
holotoxin[b]	3 ± 1	10 ± 2	43	55 ± 0.5
catalytic domain	0.7 ± 0.3	ND	25	51 ± 0.6

[a] Comparison of the functional and structural properties exhibited by unphosphorylated and phosphorylated native BoNT E and its recombinant catalytic domain. [b]Values corresponding to the proteolytic activity were taken from (*10*), and data for the protein structure and stability were from (*11*). Values are given as mean ± SEM [N (number of experiments) ≥ 2]. ND denotes not determined.

$t \geq 60$ min. These observations indicate that the BoNT E catalytic domain is substantially phosphorylated in tyrosine residues.

It has been reported that tyrosine phosphorylation of clostridial neurotoxins increases their catalytic activity and thermal stability (*10, 11*). Thus, we next investigated the functional consequences of rBoNT E LC phosphorylation by Src. For these experiments, we used rBoNT E catalytic domain phosphorylated (P) for 60 min at 30 °C with Src kinase (Figure 3A, lane 6). Unphosphorylated samples (U) denote rBoNT E LC incubated with the kinase (60 min at 30 °C) in the absence of ATP. As illustrated in Figure 3C, tyrosine phosphorylation of recombinant endopeptidase did not affect its concentration dependence of rSNAP-25 cleavage. Both unphosphorylated and phosphorylated catalytic domain forms truncated rSNAP-25 with a half-maximum concentration of ≈0.6 nM (Figure 3D, Table 1). Likewise, covalent modification of rBoNT E LC did not alter the time dependence of proteolysis nor the enzyme kinetics (data not shown).

To study the heat lability of unphosphorylated and phosphorylated proteolytic activity, we incubated both enzyme forms, U and P, for 60 min at temperatures ranging from 40 to 60 °C prior to substrate cleavage. As shown in Figure 3E, the catalytic activity of unphosphorylated species was abrogated at $T \geq 44$ °C (Figure 3E), which is lower than that reported in Figure 2G, suggesting that the 60 min phosphorylation reaction at 30 °C, prior to the temperature-induced inactivation, partially destabilizes the enzyme. In contrast, phosphorylated rBoNT E catalytic domain completely inactivated at $T \geq 48$ °C, i.e., 3−4 °C higher temperature. Therefore, tyrosine phosphorylation appears to thermally stabilize the catalytic domain without affecting its proteolytic activity.

Tyrosine Phosphorylation of the BoNT E Catalytic Domain Increases Its Helical Content and Unfolding Temperature. Because covalent modification of botulinum neurotoxins modulates structural features (*11*), we wondered if phosphorylation of the catalytic domain was also changing its secondary structure components. The circular dichroic spectra in the far-UV were obtained for unphosphorylated and phosphorylated recombinant enzymes (Figure 4A). The shapes of the CD spectra of both unphosphorylated and phosphorylated forms are practically indistinguishable, exhibiting negative double CD maxima at 207 and 222 nm and a positive maximum around 190 nm, consistent with the presence of an α-helical component (*18*). The most evident difference between both CD spectra is given by the intensity of the molar ellipticities (θ) for both negative maxima: 6330 and 8370 deg cm^2 dmol^{-1} at 207 nm, and 5825 and 7990 deg cm^2 dmol^{-1} at 222 nm for unphosphorylated and phosphorylated forms, respectively. The apparent secondary structures inferred from curve-fitting analysis of the CD spectra were 18% α-helix and 27% β-pleated sheets, and 55% of nonstructured components including random coils and turns. These values are similar to estimates for the catalytic domains of clostridial neurotoxin A and tetanus neurotoxin, and are in good agreement with those observed in the crystal structure of BoNT A and B (*24*−*30*). The most significant change induced by tyrosine phosphorylation was the increase from 18% to 25% in the α-helical content of the catalytic domain. Accordingly, tyrosine phosphorylation appears to induce a disorder-to-order transition in the structure of the catalytic domain, as evidenced by the ≈35% increment in α-helical secondary structure.

CD spectra are sensitive to structural changes caused by denaturing treatments such as heat, thus providing an operational assay to study protein stability. Both unphosphorylated and phosphorylated LC forms displayed the virtual disappearance of the CD signal upon increasing the temperature to 70 °C (Figure 4B,C, spectra b). The heat-induced unfolding process was irreversible as evidenced by the lack of recovery of the initial spectral shape upon cooling the heated samples back to 7 °C (Figure 4B,C, spectra c). To further evaluate the thermal stability of unphosphorylated and phosphorylated rBoNT E LC forms, we studied the variation of θ_{222} as a function of temperature (Figure 4D). The temperature-dependent changes of the molar ellipticity were well described by a sigmoidal curve with an inflection point corresponding to the denaturing temperature (T_d) (*11, 18*). Whereas unphosphorylated catalytic domain denaturated at 47.0 ± 0.7 °C, the phosphorylated form unfolded at 51.0 ± 0.6 °C; i.e., tyrosine phosphorylation increased the denaturation temperature by 4 °C. This value is similar to the T_d estimated from the heat-inactivating catalytic activity experimental paradigm (Figure 3E). Thus, the apparent higher order structural conformation of the catalytic domain promoted by tyrosine phosphorylation is characterized by higher thermostability.

The BoNT E Catalytic Domain Contains a Single Phosphorylation Site. Tyrosine phosphorylation of clostridial neurotoxins appears to be a common covalent modification, thus suggesting the presence of a conserved structural motif containing the phosphate acceptor site(s) (*10*). Tyrosines Y67, Y68, and Y306 in the BoNT E catalytic domain are conserved among botulinum neurotoxins, and appear to be located in phosphorylation site motifs for tyrosine kinases (Figure 1). We used site-directed mutagenesis to change these tyrosine residues to phenylalanine. As illustrated in Figure 5A, mutation of Y306 to F (Y306F) gave rise to an endopeptidase mutant that was phosphorylated by Src (Figure 5A, lane 4). In contrast, simultaneous replacement of Y67 and Y68 by F (Y67F/Y68F) produced recombinant enzyme species that were not covalently modified by incubation with Src plus ATP (Figure 5A, lane 2). Replacement of Y68 by F (Y68F) did not affect phosphorylation of the neurotoxin,

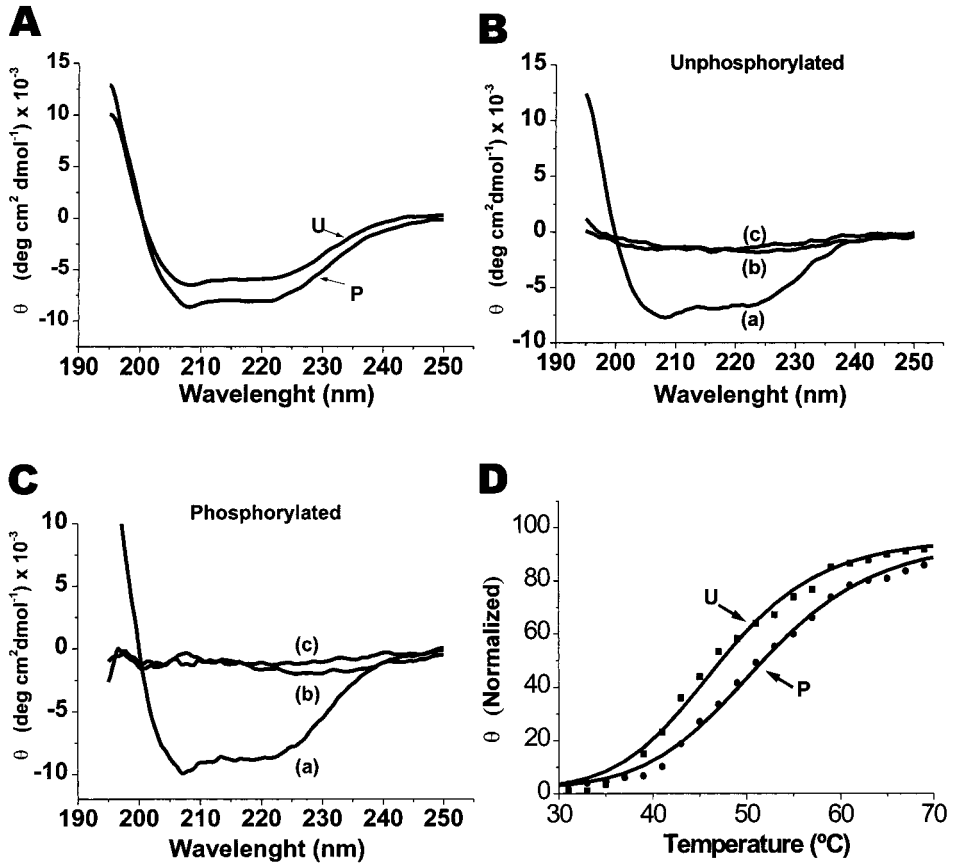

FIGURE 4: Tyrosine phosphorylation increases the percent α-helix structure and the protein thermal stability. (A) CD spectra of unphosphorylated (U) and tyrosine-phosphorylated (P) BoNT E LC at 16 °C. (B and C) CD spectra showing thermal denaturation of unphosphorylated and phosphorylated BoNT E LC, respectively. Spectra were recorded sequentially at 6 (a), 75 (b), and 6 °C (c). (D) Solid lines depict the best fit to a sigmoidal curve (see Experimental Procedures). Denaturing temperature (T_d) values were 47 ± 0.7 and 51 ± 0.6 °C, while *n* (slope of the sigmoid) values were 7.8 ± 1 and 7.9 ± 0.7 for unphosphorylated and phosphorylated BoNT E LCs, respectively. All measurements were done with 2 μM BoNT E LC in 10 mM Tris-HCl, pH 7.4, 0.05% OG. The shape of the rBoNT E LC CD spectra was not changed by the presence of either src kinase or ATP (data not shown). CD spectra represent the average of five scans, and were corrected for the buffer contribution.

while mutation of Y67 to F (Y67F) completely abolished tyrosine phosphorylation of the BoNT E catalytic domain, indicating that tyrosine 67 is the phosphate acceptor site. Consistent with this finding, the structure of BoNT A and B LCs illustrates that the uncovered, conserved phosphorylation site (Figure 1) is exposed to the solvent and thus accessible to tyrosine kinases (Figure 6) (*28*−*30*).

The enzymatic activity and thermostability of the constitutively unphosphorylated Y67F and Y67F/Y68F endopeptidase mutants resembled those characteristic of the nonphosphorylated wild-type catalytic domain (Figure 5B−E). The half-maximum concentration of mutant proteins required to cleave rSNAP-25 was 0.5 and 0.7 for Y67 and Y67F/Y68F (Figure 5B−D). The proteolytic activity of both neurotoxins thermally inactivated at $T \geq 44$ °C (Figure 5E). These observations imply that elimination of the tyrosine phosphorylation site did not alter the functionality nor the thermostability of the BoNT E catalytic domain.

DISCUSSION

We previously found that tyrosine phosphorylation of native clostridial neurotoxins significantly modulates important functional and structural properties. Because those experiments used native holotoxins, they could not provide conclusive information on the specific modulation of the neurotoxin catalytic domain by tyrosine phosphorylation (*10, 11*). We addressed this knowledge gap and used the recombinant BoNT E catalytic domain to ascertain the role of its phosphorylation on tyrosine residues. As summarized in Table 1, the salient contribution of our study is that the BoNT E catalytic domain is phosphorylated in a single tyrosine, and that covalent modification of this site augments the enzyme thermal stability without affecting its catalytic activity. This finding contrasts with the conspicuous stimulation of the proteolytic activity induced by tyrosine phosphorylation of native neurotoxins (Table 1) (*10*). This disparity may reflect conformational differences between the recombinant and native catalytic domains. Alternatively, it may also be plausible that covalent modification of the native neurotoxin increases the exposure of the LC catalytic site or modulates its dissociation from the holotoxin, rather than augmenting its enzymatic activity. It is already known that reduction of the disulfide bond linking the two neurotoxin chains does not suffice to fully dissociate both neurotoxin chains (*1, 31*). Hence, incorporation of negative charges in both neurotoxin domains could destabilize their interaction and facilitate the release of the catalytic domain (*31*). Accordingly, the lower half-maximum concentration and shorter times needed by the phosphorylated endopeptidase to truncate SNAP-25 would reflect an increase in the

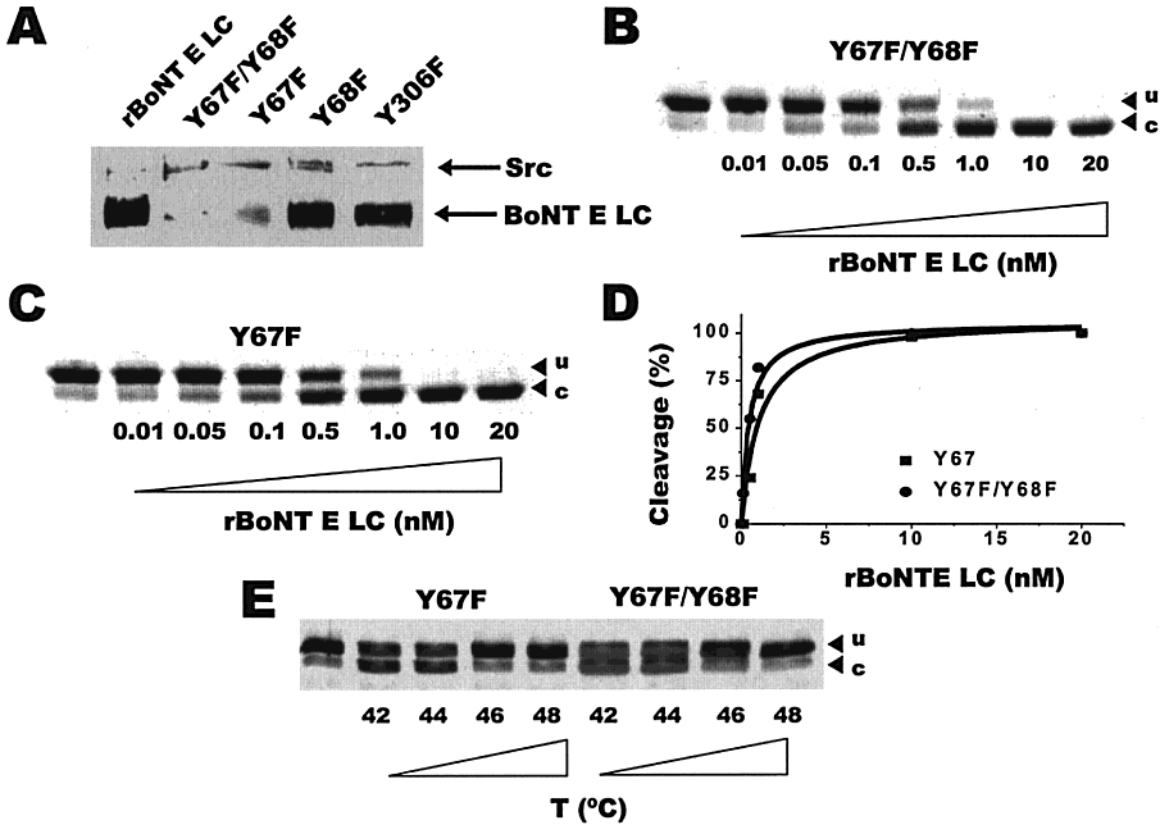

FIGURE 5: BoNT E catalytic domain is phosphorylated at a single phosphate acceptor site. (A) Mutation of Y67 to F (Y67F) completely abolishes tyrosine phosphorylation of BoNT E LC by Src. Western immunoblot probed with an anti-phosphotyrosine monoclonal antibody. Proteins were phosphorylated with 9 units of kinase, for 60 min at 30 °C. (B and C) Cleavage of rSNAP-25 as a function of the concentration of Y67F/Y68F and Y67F endopeptidase mutants, respectively. (D) Extent of rSNAP-25 proteolysis quantified from the gels shown in panels B and C and plotted as a function of enzyme concentration. (E) Thermal inactivation of the catalytic activity of the constitutively unphosphorylated Y67F and Y67F/Y68F mutants. Enzyme mutants were incubated with Src kinase and ATP for 60 min at 30 °C, incubated for 60 min at the indicated temperatures, and assayed for proteolysis of rSNAP-25. The rSNAP-25 concentration was 6 μM. The cleavage reaction was carried out for 5 min at 23 °C. The first lane in panel E denotes rSNAP-25 in the absence of enzyme.

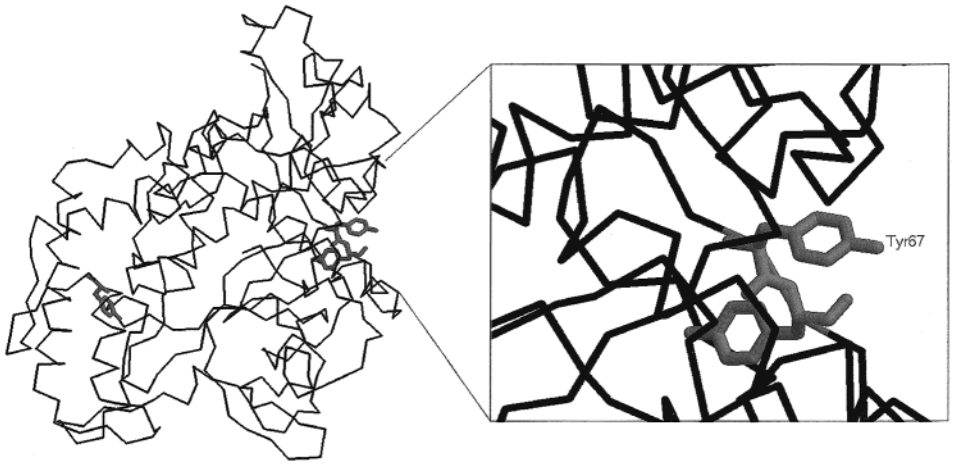

FIGURE 6: Tyrosine 67 in the catalytic domain appears exposed to the solvent and accessible to tyrosine kinases. (Left) The crystal structure of BoNT A LC taken from the PDB [accession number 3BTA (*28*)]. Highlighted in boldface are Y71 and Y72 (corresponding to Y67 and Y68 in BoNT E LC, Figure 1) and Y320 (corresponding to Y306 in BoNT E LC, Figure 1). (Right) The region containing the phosphate acceptor site (labeled as Y67 for clarity) is shown enlarged. The RasMol program was used to generate the figure.

effective enzyme concentration. This tenet is consistent with our finding that the unphosphorylated recombinant catalytic domain exhibits 10-fold higher efficacy cleaving SNAP-25 than the native neurotoxin (Table 1).

The higher thermostability of the phosphorylated catalytic domain appears to be associated with alterations in the secondary structure, primarily a 35% increase in the α-helical content presumably concomitant to a decrease in random structures. The magnitude of this disorder-to-order transition and thermostabilization closely resembles that observed for the phosphorylated form of the native neurotoxin (Table 1), suggesting that the structural change in the phosphorylated holotoxin may arise significantly from the higher order acquired by the catalytic domain. Likewise, the virtually identical phosphorylation-induced increase of the denaturation temperature of the recombinant catalytic domain and

native neurotoxin implies an important contribution of the catalytic domain to the overall higher thermal stability of the holotoxin (Table 1). Further studies are necessary to precisely understand the nature of the interaction between the HC and the catalytic domain.

Our results demonstrate the presence of a single phosphate acceptor site at position 67 of the N-end of the catalytic domains. Replacement of tyrosine by phenylalanine created constitutively unphosphorylated catalytic domains with functional properties and thermostability similar to those exhibited by the nonphosphorylated form of the enzyme. The question that arises is the following: How could phosphorylation of tyrosine 67 modulate the structure and thermostability of the catalytic domain? Although the crystal structure of BoNT E is yet unknown, it is reasonable to consider the BoNT A structure as representative for all clostridial neurotoxins (*12*, *28*). This notion is substantiated by the similarity of the recently reported crystal structure of BoNT B and its LC to BoNT A (*28*−*30*). The three-dimensional structure of BoNT A at 3.0 Å and BoNT B at 2.0 Å shows the catalytic domain as a mixture of both α-helix and β-strand secondary structure, consistent with our estimates and those reported by others (*28*−*30*). The catalytic site is buried 20−40 Å deep in the protein, being accessible by a channel bordered by three flexible loops that comprise residues 47−80 (loop B), residues 231−259 (loop C), and residues 356−371 (loop D) (*12*, *27*−*29*). The phosphate acceptor site, Y67, is located in loop B and solvent-accessible (Figure 6). Although the crystal structure of BoNT A LC does not reveal an important role for Y67, its location in a flexible loop close to the catalytic site implies that incorporation of a negative charge may structure this segment and compact the protein, thus increasing the thermostability (*32*, *33*). The flexibility of this protein domain has been recently illustrated by the structural differences observed in loop B between the unbound BoNT B LC and that complexed to synaptobrevin (*29*). This notion is also supported by the change in the degree of disorder upon phosphorylation, and by the observation that surface residues may critically contribute to the thermostability of a protein as reported for thermophilic proteins (*34*). Interestingly, the only apparent structural difference between mesophilic and thermophilic proteins seems to be that thermophilic proteins have more salt bridges on their surfaces, thus relying on additional polar interactions for their greater stability (*16*). Hence, incorporation of a charged group at Y67 might change the number of surface polar interactions, thus increasing the stability of the protein. Nonetheless, the precise structural modulation exerted by phosphorylation will have to be addressed by determining the structure of both the unphosphorylated and phosphorylated forms.

These findings, along with previous reports (*10*), suggest that the biologically active form of the catalytic domain inside the cells might be phosphorylated on tyrosine residues. Hence, tyrosine phosphorylation of the catalytic domain might contribute to the long-lasting paralytic effects exerted by BoNTs in botulism or in their therapeutic application. However, further experimental support is required to fully understand the biological relevance of BoNTs covalent modification by intracellular signaling cascades that promote tyrosine phosphorylation. Our results suggest that modifications of the catalytic domain that emulate the phosphorylated form may provide a feasible approach to design enzyme species with higher thermostability and improved clinical utility.

ACKNOWLEDGMENT

We are indebted to Heiner Niemann for providing the BoNT E LC cDNA. We thank Mauricio Montal, José Manuel González-Ros, José A. Ferragut, and Marco Caprini for insightful comments on the manuscript.

REFERENCES

1. Simpson, L. L. (1981) *Pharmacol. Rev. 33*, 155−187.
2. Montecucco, C., and Schiavo, G. (1994) *Mol. Microbiol. 13*, 1−8.
3. Ahnert-Hilger, J., and Bigalke, H. (1995) *Prog. Neurobiol. 46*, 83−96.
4. Jankovic, J., and Hallet, M., Eds. (1994) *Therapy with botulinum toxin*, Marcel Dekker, New York.
5. Schiavo G., Benfenati, F., Poulain, B., Rossetto, O., Polverino de Laureto, P., DasGupta, B. R., and Montecucco, C. (1992) *Nature 359*, 832−835.
6. Blasi, J., Chapman, E. R., Link, E., Binz, T., Yamasaki, S., De Camilli, P., Sudhof, T. C., Niemann, H., and Jahn, R. (1993) *Nature 365*, 160−163.
7. Hayashi, T., McMahom, H., Yamasaki, S., Binz, T., Hata, Y., Sudhof, T. C., and Niemann, H. (1994) *EMBO J. 13*, 5051−5061.
8. Janh, R., and Sudhof, T. C. (1994) *Annu. Rev. Neurosci. 17*, 219−246.
9. Scheller, R. H. (1995) *Neuron 14*, 893−897.
10. Ferrer-Montiel, A. V., Canaves, J. M., DasGupta, B. R., Wilson, M. C., and Montal, M. (1996) *J. Biol. Chem. 271*, 18322−18325.
11. Encinar, J. A., Fernández, A., Ferragut, J. A., González-Ros, J. M., DasGupta, B. R., Montal, M., and Ferrer-Montiel, A. V. (1998) *FEBS Lett. 429*, 78−82.
12. Lacy, B., and Stevens, R. Y. (1999) *J. Mol. Biol. 291*, 1091−1104.
13. Paulet, S., Hauser, D., Quanz, M., Niemann, H., and Popoff, M. R. (1992) *Biochem. Biophys. Res. Commun. 183*, 107−113.
14. Ferrer-Montiel, A. V., and Montal, M. (1999) *Methods Mol. Biol. 128*, 167−178.
15. Ferrer-Montiel, A. V., Sun, W., and Montal, M. (1995) *Proc. Natl. Acad. Sci. U.S.A. 92*, 8021−8025.
16. Creighton, T. E. (1993) in *Proteins: Structures and Molecular Properties*, W. H. Freemann and Co., New York.
17. Geourjon, C., and Deleage, G. (1995) *J. Mol. Graphics 13*, 209−212.
18. Woody, R. W. (1995) *Methods Enzymol. 246*, 34−71.
19. Vaidyanathan, V. V., Yoshino, K., Jahnz, M., Dorries, C., Bade, S., Nauenburg, S., Niemann, H., and Binz, T. (1999) *J. Neurochem. 72*, 327−337.
20. Zhou, L., De Pavia, A., Liu, D., Aoki, R., and Dolly, J. O. (1995) *Biochemistry 34*, 15175−15181.
21. Li, L., and Singh, B. R. (1999) *Protein Expression Purif. 17*, 339−344.
22. Tonello, F., Pellizzari, R., Pasqualato, S., Grandi, G., Peggion, E., and Montecucco, C. (1999) *Protein Expression Purif. 15*, 221−227.
23. Dasgupta, B. R., and Tepp, W. (1991) *Soc. Neurosci. Abstr. 17*, 1526.
24. Singh, B. R., and DasGupta, B. R. (1990) *Biophys. Chem. 38*, 123−130.
25. Lebeda, F. J., and Olson, M. A. (1994) *Proteins: Struct., Funct., Genet. 20*, 293−300.
26. De Filippis, V., Vangelista, L., Schiavo, G., Tonello, F., and Montecucco, C. (1995) *Eur. J. Biochem. 229*, 61−69.
27. Li, L., Binz, T., Niemann, H., and Singh, B. R. (2000) *Biochemistry 39*, 2399−2405.

28. Lacy, D. B., Tepp, W., Cohen, A. C., DasGupta, B. R., and Stevens, R. C. (1998) *Nat. Struct. Biol. 5*, 898−902.
29. Hanson, M. A., and Stevens, R. C. (2000) *Nat. Struct. Biol. 7*, 687−692.
30. Swaminathan, S., and Eswaramoorthy, S. (2000) *Nat. Struct. Biol. 7*, 693−699.
31. Johnson, L. N., and Barford, D. (1993) *Annu. Rev. Biophys. Biomol. Struct. 22*, 199−29.
32. Johnson, L. N., and O'Relly, M. (1996) *Curr. Opin. Struct. Biol. 6*, 762−769.
33. Perl, D., Mueller, U., Heinemann, U., and Schimd, F. (2000) *Nat. Struct. Biol. 7*, 380−383.
34. Cooper, J. A., Esch, F. S., Taylor, S. S., and Hunter, T. (1984) *J. Biol. Chem. 259*, 7835−7841.

BI001919Y